

Fast Beam Alignment for Millimeter Wave Communications: A Sparse Encoding and Phaseless Decoding Approach

Xingjian Li, Jun Fang, Huiping Duan, Zhi Chen, and Hongbin Li, *Senior Member, IEEE*

Abstract—In this paper, we studied the problem of beam alignment for millimeter wave (mmWave) communications, in which we assume a hybrid analog and digital beamforming structure is employed at the transmitter (i.e. base station), and an omni-directional antenna or an antenna array is used at the receiver (i.e. user). By exploiting the sparse scattering nature of mmWave channels, the beam alignment problem is formulated as a sparse encoding and phaseless decoding problem. More specifically, the problem of interest involves finding a sparse sensing matrix and an efficient recovery algorithm to recover the support and magnitude of the sparse signal from compressive phaseless measurements. A sparse bipartite graph coding (SBG-Coding) algorithm is developed for sparse encoding and phaseless decoding. Our theoretical analysis shows that, in the noiseless case, our proposed algorithm can perfectly recover the support and magnitude of the sparse signal with probability exceeding a pre-specified value from $\mathcal{O}(K^2)$ measurements, where K is the number of nonzero entries of the sparse signal. The proposed algorithm has a simple decoding procedure which is computationally efficient and noise-robust. Simulation results show that our proposed method renders a reliable beam alignment in the low and moderate signal-to-noise ratio (SNR) regimes and presents a clear performance advantage over existing methods.

Index Terms—Millimeter wave (mmWave) communications, beam alignment, sparse encoding and phaseless decoding.

I. INTRODUCTION

Millimeter wave (mmWave) communication is a promising technology for future cellular networks [1]–[4]. It has the potential to offer gigabits-per-second communication data rates by exploiting the large bandwidth available at mmWave frequencies. Nevertheless, communication at the mmWave frequency bands suffers from high attenuation and signal absorption [5]. To address this issue, large antenna arrays should be used to provide sufficient beamforming gain for mmWave communications [6]. In fact, thanks to the small wavelength at the mmWave frequencies, the antenna size is very small and thus a large number of array elements can be

packed into a small area, which makes the use of large antenna arrays a feasible option for mmWave communications.

On the other hand, although directional beamforming helps compensate for the significant path loss incurred by mmWave signals, it comes up with a complicated beamforming training procedure because, due to the narrow beam of the antenna array, communication between the transmitter and the receiver is possible only when the transmitter’s and receiver’s beams are well-aligned, i.e. the beam directions are pointing towards each other. Therefore, beamforming training is required to find the best beamformer-combiner pair that gives the highest beamforming gain [7]. A natural approach to perform beamforming training is to exhaustively search for all possible beam pairs to identify the best beam alignment, which requires the receiver to scan the entire space for each choice of beam direction on the transmitter side. This exhaustive search has a sample complexity of $\mathcal{O}(N^2)$ (N denotes the number of possible beam directions) and usually takes a long time (up to several seconds) to converge, particularly when the number of antennas at the transmitter and the receiver is large [8].

To address this issue, many efforts have been made to reduce the time required for beamforming training. Specifically, the IEEE 802.11ad standard proposed to conduct an exhaustive search at the receiver, with the transmitter adopting a quasi-omnidirectional beam pattern. This process is then reversed to have the transmitter sequentially scan the entire space while the receiver uses a quasi-omnidirectional beam shape. This protocol reduces sample complexity from $\mathcal{O}(N^2)$ to $\mathcal{O}(N)$. To further reduce the training time, adaptive beam alignment algorithms, e.g. [9]–[13], were proposed. In these works, a hierarchical multi-resolution beamforming codebook set is employed to avoid the costly exhaustive sampling of all pairs of transmit and receive beams. The basic idea is to use coarse codebooks to first identify the range of the beam direction, and then use high-resolution subcodebooks to find a finer beam direction. This adaptive beam alignment requires to adaptively choose a subcodebook at each stage based on the output of earlier stages, which requires feedback from the receiver to the transmitter and may not be available at the initial channel acquisition stage.

In addition to the above beam steering techniques, another approach [14]–[23] directly estimates the mmWave channel or its associated parameters, e.g. angles of arrival/departure, without the need of scanning the entire space. The rationale behind this class of methods is to exploit the sparse scattering nature of mmWave channels and formulate the channel esti-

Xingjian Li, Jun Fang and Zhi Chen are with the National Key Laboratory of Science and Technology on Communications, University of Electronic Science and Technology of China, Chengdu 611731, China, Email: Jun-Fang@uestc.edu.cn

Huiping Duan is with the School of Electronic Engineering, University of Electronic Science and Technology of China, Chengdu 611731, China, Email: huipingduan@uestc.edu.cn

Hongbin Li is with the Department of Electrical and Computer Engineering, Stevens Institute of Technology, Hoboken, NJ 07030, USA, E-mail: Hongbin.Li@stevens.edu

This work was supported in part by the National Science Foundation of China under Grant 61522104.

mation into a compressed sensing problem. Although having the potential to substantially reduce the training overhead, this compressed sensing-based approach suffers from several drawbacks. Firstly, compressed sensing methods usually involve a computational complexity that might be too excessive for practical systems. Secondly, compressed sensing methods require the knowledge of the phase of the measurements. While in mmWave communications, due to the carrier frequency offset (CFO) caused by high-frequency hardware imperfections, the phase of the measurements might be corrupted by a random noise that varies across time, and as a result, only the magnitude information of the measurements is useful for beam alignment. Lastly, for compressed sensing methods, the beamforming/combining vectors have to be chosen to be random vectors to satisfy the restricted isometry property. This, however, comes at the cost of worse signal-to-noise ratio (SNR) and reduced transmission range. Recently, a novel beam steering scheme called as ‘‘Agile-Link’’ [8], [24] was proposed to find the correct beam alignment. The proposed algorithm only uses the magnitude information of the measurements for recovery of the signal directions and achieves a sample complexity of $\mathcal{O}(K \log N)$, where K denotes the number of signal paths.

In this paper, we continue the efforts towards developing a fast and efficient beam alignment scheme for mmWave communications. Similar to [8], [24], we rely on the magnitude information of the measurements for beam steering. By exploiting the sparse scattering nature of mmWave channels, we show that the beam alignment problem can be formulated as a sparse encoding and phaseless decoding problem. More specifically, the problem of interest is to devise a sparse sensing matrix \mathbf{A} (referred to as sparse encoding) and develop a fast and efficient recovery algorithm (referred to as phaseless decoding) to recover the support and magnitude information of the sparse signal \mathbf{x} from compressive phaseless measurements:

$$\mathbf{y} = |\mathbf{A}\mathbf{x}| \quad (1)$$

Note that the estimation of sparse signals from compressive phaseless measurements, termed as ‘‘compressive phase retrieval (CPR)’’, has been extensively studied over the past few years, e.g. [25]–[28]. Nevertheless, there are two important distinctions between our problem and the standard CPR problem. First, standard CPR assumes a random measurement matrix which satisfies the restricted isometry property. For our problem, the measurement matrix which determines the shape of the beam pattern cannot be designed freely. In fact, to provide a sufficient beamforming gain for signal reception, we need to impose a sparse structure on the measurement matrix. Second, standard CPR aims to retrieve the complete information of the sparse signal \mathbf{x} , while for the beam alignment purpose, only partial information of \mathbf{x} , i.e. the support and the magnitude information of those nonzero entries, needs to be recovered.

To our best knowledge, in existing literature, PhaseCode proposed in [29] is a CPR algorithm that is most relevant to our sparse encoding and phaseless decoding problem, in which its measurement matrix is devised based on a sparse-graph coding framework. It was shown that PhaseCode can recover a K -sparse signal using slightly more than $4K$ measurements

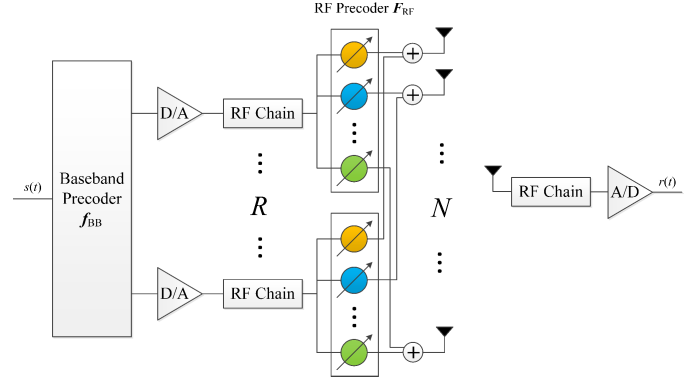


Fig. 1. The transmitter has a hybrid beamforming structure, and the receiver uses an omni-directional antenna.

with high probability. Nevertheless, PhaseCode (even its robust version) involves a delicate decoding procedure sensitive to noise and measurement errors, and suffers from severe performance degradation in the presence of noise. To overcome this difficulty, in this work, we propose a sparse bipartite graph code (SBG-Code) algorithm for sparse encoding and phaseless decoding. Different from PhaseCode, our proposed method uses a set of sparse bipartite graphs, instead of a single bipartite graph, to encode the sparse signal. The proposed algorithm involves a simple decoding procedure which has a minimum computational complexity and is robust against noise. Also, it can recover the support and magnitude information of a K -sparse signal with a sample complexity of $\mathcal{O}(K^2)$, thus providing a competitive solution for practical mmWave beam alignment systems.

The rest of the paper is organized as follows. In Section II, the system model is discussed and the beam alignment is formulated into a sparse encoding and phaseless decoding problem. In Section III, an overview of PhaseCode is provided. A SBG-Code method is developed in Section IV, along with its theoretical analysis provided in V. The robust version of SBG-Code is studied in VI and the extension to antenna array receiver is discussed in Section VII. Simulation results are provided in Section VIII, followed by concluding remarks in Section IX.

II. SYSTEM MODEL

Consider a mmWave communication system which consists of a transmitter (base station) and a receiver (user). We assume that a hybrid analog and digital beamforming structure is employed at the transmitter, while the receiver has an omni-directional antenna that receives in all directions (see Fig. 1). The extension to an antenna array receiver will be discussed in Section VII. The transmitter is equipped with N antennas and R RF chains. Since the RF chain is expensive and power consuming, we have $R \ll N$. Note that although a single receiver is considered in our paper, the extension of our scheme to the multi-user scenario is straightforward, in which case the base station periodically broadcasts a common codeword that is decoded by each user to extract its associated

channel information [30]. Each user then sends the index of the beam corresponding to the selected angle-of-departure (AoD) to the base station via a random access control channel. A connection between the base station and the user is established after the user receives a response from the base station.

The mmWave channel is characterized by a geometric channel model [11]

$$\mathbf{h} = \sum_{p=1}^P \alpha_p \mathbf{a}_t(\theta_p) \quad (2)$$

where P is the number of paths, α_p is the complex gain associated with the p th path, $\theta_p \in [0, 2\pi]$ is the associated azimuth angle of departure (AoD), and $\mathbf{a}_t \in \mathbb{C}^N$ is the transmitter array response vector. Suppose a uniform linear array (ULA) is used. Then the steering vector at the transmitter can be written as

$$\mathbf{a}_t(\theta_p) = \frac{1}{\sqrt{N}} \left[1, e^{j\frac{2\pi}{\lambda}d \sin(\theta_p)}, \dots, e^{j(N-1)\frac{2\pi}{\lambda}d \sin(\theta_p)} \right]^T \quad (3)$$

where λ is the signal wavelength, and d is the distance between neighboring antenna elements. Due to the sparse scattering nature of mmWave channels, \mathbf{h} has a sparse representation in the beam space (angle) domain:

$$\mathbf{h} = \mathbf{D}\mathbf{x} \quad (4)$$

where $\mathbf{D} \in \mathbb{C}^{N \times N}$ is the discrete Fourier transform (DFT) matrix, and $\mathbf{x} \in \mathbb{C}^N$ is a K -sparse vector. If the true AoA parameters $\{\theta_p\}$ lie on the discretized grid specified by the DFT matrix, then the number of nonzero entries in the beam space domain equals the number of signal paths, i.e. $K = P$. The objective of beam alignment is to estimate the AoD and the attenuation (in magnitude) of each path, which is equivalent to recover the location indices and the magnitudes of the nonzero entries in \mathbf{x} . The AoD of the dominant path is then reported back to the base station via a control channel for beam alignment.

Suppose the transmitter sends a constant signal $s(t) = 1$ to the receiver. The signal received at the t th time instant can be expressed as

$$r(t) = \mathbf{h}^T \mathbf{b}(t) s(t) + w(t) = \mathbf{x}^T \mathbf{D}^T \mathbf{b}(t) + w(t) \quad (5)$$

where $\mathbf{b}(t) \in \mathbb{C}^N$ is the precoding/beamforming vector used by the transmitter at the t th time instant, and $w(t)$ denotes the additive complex Gaussian noise with zero mean and variance σ^2 . Since a hybrid analog and digital beamforming structure is employed at the transmitter, the precoding vector can be expressed as

$$\mathbf{b}(t) = \mathbf{F}_{\text{RF}}(t) \mathbf{f}_{\text{BB}}(t) \quad (6)$$

in which $\mathbf{F}_{\text{RF}}(t) \in \mathbb{C}^{N \times R}$ and $\mathbf{f}_{\text{BB}}(t) \in \mathbb{C}^R$ represent the radio frequency (RF) precoding matrix and the baseband (BB) precoding vector, respectively. Specifically, to provide a sufficient beamforming gain for signal reception, the transmitter needs to form multiple beams simultaneously and steers them towards different directions. To this objective, the RF

precoding matrix is chosen to be a submatrix of the complex conjugate of the DFT matrix, \mathbf{D}^*

$$\mathbf{F}_{\text{RF}}(t) = \mathbf{D}^* \mathbf{S}(t) \quad (7)$$

where $\mathbf{S}(t) \in \mathbb{R}^{N \times R}$ is a column selection matrix containing only one nonzero entry per column. Note that each column of the DFT matrix can be considered as a beamforming vector steering a beam to a certain direction. Hence, the RF precoding matrix defined in (7) forms R beams towards different directions simultaneously.

Substituting (6)–(7) into (5), we obtain

$$r(t) = \mathbf{x}^T \mathbf{a}(t) + w(t) = \mathbf{a}^T(t) \mathbf{x} + w(t) \quad (8)$$

where $\mathbf{a}(t) \triangleq \mathbf{S}(t) \mathbf{f}_{\text{BB}}(t)$ is an N -dimensional sparse vector with at most R nonzero elements. It should be noted (8) is an ideal model without taking the CFO effect into account. In mmWave communications, CFO is a factor that cannot be neglected, and, due to the CFO between the transmitter and the receiver, the measurements $r(t)$ will incur an additional unknown phase shift that varies across time [8]. Correcting this unknown phase shift is difficult due to the high frequencies of mmWave signals. In this case, only the magnitude information of the measurements $r(t), t = 1, \dots, T$ is reliable.

Our objective is to devise a measurement matrix $\mathbf{A} \triangleq [\mathbf{a}(1) \dots \mathbf{a}(T)]^T \in \mathbb{C}^{T \times N}$ (referred to as sparse encoding) and develop a fast and efficient recovery algorithm (referred to as phaseless decoding) to recover $\mathbf{z} = |\mathbf{x}|$, i.e. the support and magnitude of the sparse signal \mathbf{x} , from compressive phaseless measurements:

$$\mathbf{y} \triangleq |\mathbf{r}| = |\mathbf{A}\mathbf{x} + \mathbf{w}| \quad (9)$$

where $\mathbf{r} \triangleq [r(1) \dots r(T)]^T$, and $\mathbf{w} \triangleq [w(1) \dots w(T)]^T$. Note that the measurement matrix \mathbf{A} cannot be designed freely. As discussed earlier, the transmitter has to form directional beams for signal reception, otherwise the power of the signal may be too weak to be received. To meet such a requirement, a sparse structure is placed on \mathbf{A} :

C1 \mathbf{A} is a sparse matrix with each row of \mathbf{A} containing at most R nonzero elements.

For this reason, the design of the measurement matrix \mathbf{A} is referred to as sparse encoding. Also, since the amount of time for beamforming training is proportional to the number of measurement T , we wish \mathbf{A} is properly devised such that a reliable estimate of $\mathbf{z} = |\mathbf{x}|$ can be obtained by using as few measurements as possible.

III. REVIEW OF EXISTING SOLUTIONS

PhaseCode [29] is a CPR algorithm that is most relevant to our sparse encoding and phaseless decoding problem. Here we first provide a brief review on PhaseCode. PhaseCode is an efficient algorithm developed in a sparse-graph coding framework. It consists of an encoding step and a decoding step. In the encoding step, the measurement matrix $\mathbf{A} \in \mathbb{C}^{4M \times N}$ is devised according to

$$\mathbf{A} \triangleq \mathbf{H} \odot \bar{\mathbf{T}} \quad (10)$$

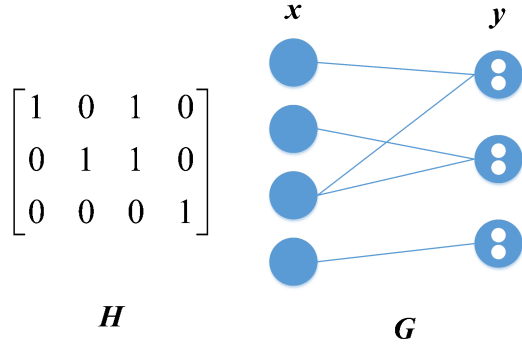


Fig. 2. The bipartite graph G and its associated binary code matrix \mathbf{H} , in which each left node of G corresponds to an component of \mathbf{x} , and each right node of G corresponds to the set of measurements obtained via the corresponding row of \mathbf{H} .

where \odot denotes the Khatri-Rao product, $\mathbf{H} \in \{0, 1\}^{M \times N}$ is a binary code matrix constructed using a random bipartite graph G with N left nodes and M right nodes, with its (i, j) th entry $H(i, j) = 1$ if and only if left node j is connected to right node i , otherwise $H(i, j) = 0$. $\bar{\mathbf{T}} \in \mathbb{C}^{4 \times N}$ is the so-called “trigonometric modulation” matrix that provides 4 measurements for each row of \mathbf{H} , and $\bar{\mathbf{T}}$ is given by

$$\bar{\mathbf{T}} \triangleq \begin{bmatrix} e^{j\omega} & e^{j2\omega} & \dots & e^{jN\omega} \\ e^{-j\omega} & e^{-j2\omega} & \dots & e^{-jN\omega} \\ 2 \cos(\omega) & 2 \cos(2\omega) & \dots & 2 \cos(N\omega) \\ e^{j\omega'} & e^{j2\omega'} & \dots & e^{jN\omega'} \end{bmatrix} \quad (11)$$

where $\omega \in (0, 2\pi/N]$, and ω' is a random phase between 0 and 2π . In the decoding stage, a delicate procedure is employed to recover \mathbf{x} . It was shown in [29] that, in the noiseless case, PhaseCode can recover a K -sparse signal with high probability using only slightly more than $4K$ measurements. This theoretical result suggests that the sample complexity required for beam alignment can be significantly reduced to as low as $\mathcal{O}(K)$. Nevertheless, there are two major issues when applying PhaseCode to the beam alignment problem. Firstly, in PhaseCode, the bipartite graph G used to determine the binary code matrix \mathbf{H} is randomly generated. There is no guarantee that the resulting measurement matrix \mathbf{A} satisfies constraint C1. Secondly, PhaseCode involves a delicate decoding procedure requiring a high accuracy of the measurements, and suffers from severe performance degradation in the presence of noise. This makes PhaseCode an unsuitable solution for beam alignment problems where measurements are inevitably contaminated by noise.

IV. PROPOSED SBG-CODING ALGORITHM

To overcome the drawbacks of existing solutions, we propose a sparse bipartite graph-Code (SBG-Code) algorithm for sparse encoding and phaseless decoding.

A. Sparse Encoding

Different from PhaseCode, the proposed SBG-Code uses a set of bipartite graphs $\{G_l\}_{l=1}^L$, instead of a single bipartite

graph, to encode the sparse signal. Let $\mathbf{H}_l \in \{0, 1\}^{M \times N}$ denote the binary code matrix associated with the graph G_l with N left nodes and M right nodes. The (i, j) th entry of \mathbf{H}_l is given by

$$H_l(i, j) = \begin{cases} 1 & \text{if and only if left node } j \text{ of } G_l \text{ is connected} \\ & \text{to right node } i \text{ of } G_l \\ 0 & \text{otherwise} \end{cases} \quad (12)$$

Given $\{\mathbf{H}_l\}$, the measurement matrix $\mathbf{A} \in \mathbb{R}^{2ML \times N}$ is devised as

$$\mathbf{A} \triangleq \begin{bmatrix} \mathbf{H}_1 \odot \mathbf{T} \\ \mathbf{H}_2 \odot \mathbf{T} \\ \vdots \\ \mathbf{H}_L \odot \mathbf{T} \end{bmatrix} \quad (13)$$

where $\mathbf{T} \in \mathbb{R}^{2 \times N}$ is a simplified trigonometric modulation matrix defined as

$$\mathbf{T} \triangleq \begin{bmatrix} 1 & 1 & \dots & 1 \\ 2 \cos(\omega) & 2 \cos(2\omega) & \dots & 2 \cos(N\omega) \end{bmatrix} \quad (14)$$

in which $\omega \in (0, \pi/(2N)]$ such that $\cos(\omega l) \in [0, 1)$. We will show later the trigonometric function $\cos(n\omega)$ can be replaced by a general function.

For each graph G_l , each of its left node can be deemed as a component of the sparse signal \mathbf{x} , and each right node of G_l refers to a set of 2 measurements obtained as (see Fig. 2)

$$\mathbf{y}_{l,m} = |(\mathbf{H}_l[m, :] \odot \mathbf{T})\mathbf{x}| \quad \forall m = 1, \dots, M \quad (15)$$

where $\mathbf{H}_l[m, :]$ denotes the m th row of \mathbf{H}_l . A left node, say node n , is called as active left node if the n th signal component, x_n , is nonzero. For a K -sparse signal \mathbf{x} , there are K active left nodes in total. A right node is called as a nullton, a singleton or a multiton if:

- Nullton: A right node is a nullton if it is not connected to any active left node.
- Singleton: A right node is a singleton if it is connected to exactly one active left node.
- Multiton: A right node is a multiton if it is connected to more than one active left node.

A bipartite graph which does not contain any multiton right nodes is called as

- No-Multiton-graph (NM-graph): A bipartite graph whose right nodes are either singletons or nulltons.

For our proposed SBG-Code, the purpose of employing multiple bipartite graphs is to ensure that, with overwhelming probability, there exists at least an NM-graph, i.e. a bipartite graph whose right nodes are either singletons or nulltons.

The bipartite graphs $\{G_l\}$ with N left nodes and M ($M > K$) right nodes are designed as follows. First, for simplicity, we assume $r \triangleq N/M$ to be an integer. For each graph, we randomly divide N left nodes into M equal-size, disjoint sets (i.e. each set has r left nodes) and establish a one-to-one correspondence between M sets of left nodes and M right nodes. If N is not an integer multiple of M , we can still divide N left nodes into M disjoint sets, with all sets, except

the last one, consisting of $r = \text{floor}(N/M)$ left nodes. Clearly, a right node is a singleton (nullton) if its corresponding set of left nodes contains only one (zero) active left node. As to be shown later, such design helps maximize the probability that a bipartite graph is an NM-graph, i.e. its right nodes are either singletons or nulltons. Clearly, for each bipartite graph G_l devised as described, its corresponding binary code matrix \mathbf{H}_l has only one nonzero element per column, and at most r nonzero elements per row. As a result, each row of the resulting measurement matrix \mathbf{A} contains at most r nonzero elements. We can therefore choose $r \leq R$, which is equivalent to $M \geq N/R$, such that \mathbf{A} satisfies constraint C1. Once \mathbf{A} is given, the RF precoding matrices $\{\mathbf{F}_{\text{RF}}(t)\}$ and baseband precoding vectors $\{\mathbf{f}_{\text{BB}}(t)\}$ can be accordingly determined.

B. Phaseless Decoding

Next, we discuss how to retrieve the support and magnitude information of \mathbf{x} from compressive phaseless measurement \mathbf{y} . We first ignore the observation noise in order to simplify our exposition and analysis, i.e.

$$\mathbf{y} = |\mathbf{A}\mathbf{x}| \quad (16)$$

Let

$$\mathbf{A}_l \triangleq \mathbf{H}_l \odot \mathbf{T} \quad (17)$$

denote the l th measurement sub-matrix associated with the bipartite graph G_l , and

$$\mathbf{y}_l \triangleq |\mathbf{A}_l\mathbf{x}| \quad (18)$$

denote the corresponding measurements. Suppose G_l is an NM-graph. If a right node is a nullton, it does not connect to any active left nodes and thus we have $\mathbf{y}_{l,m} = \mathbf{0}$. Therefore we only need to consider those singleton right nodes. A singleton right node means that only one nonzero component of \mathbf{x} , say x_n , contributes to the value of $\mathbf{y}_{l,m}$. More precisely, we can write

$$\mathbf{y}_{l,m} = \begin{bmatrix} |x_n| \\ |2 \cos(n\omega)x_n| \end{bmatrix} \quad (19)$$

Clearly, the magnitude and location index of x_n can be readily estimated as

$$\begin{aligned} z_{\hat{n}} &= y_{l,m}^{(1)} \\ \hat{n} &= \frac{1}{\omega} \arccos \left(\frac{y_{l,m}^{(2)}}{2y_{l,m}^{(1)}} \right) \end{aligned} \quad (20)$$

where $y_{l,m}^{(1)}$ and $y_{l,m}^{(2)}$ denote the first and second entry of $\mathbf{y}_{l,m}$, respectively. Note that the graph G_l is designed such that each right node is exclusively connected to a subset of left nodes, and every left node belongs to a certain subset that is connected to a certain right node. Therefore, by performing the estimation (20) for all singleton right nodes, we are guaranteed to find the location indices and magnitudes of all active left nodes. From the above discussion, we see that if a bipartite graph, say graph G_l , is an NM-graph, then $z = |\mathbf{x}|$ can be recovered from the corresponding phaseless measurements \mathbf{y}_l .

Algorithm 1 Proposed SBG-Code Algorithm

Given $\mathbf{A}_l = \mathbf{H}_l \odot \tilde{\mathbf{T}}$ and \mathbf{y}_l for each bipartite graph G_l , $l = 1, \dots, L$

for $l = 1, \dots, L$ **do**

for $m = 1, \dots, M$ **do**

if $\mathbf{y}_{l,m} \neq \mathbf{0}$ **then**

 Assume the m th right node is a singleton.

 Estimate the magnitude and the location index of the active left node connected to the m th right node via (20)

end if

end for

 Obtain an estimate of z , denoted as $\hat{z}^{(l)}$.

end for

Given the L estimates $\{\hat{z}^{(l)}\}_{l=1}^L$, choose the estimate that has the largest number of nonzero entries as the final estimate.

The problem is that since we do not have the support information of the sparse signal in advance, there is no guarantee that a designed graph is an NM-graph which only contains singleton and nullton right nodes. To address this issue, we employ multiple bipartite graphs to encode the sparse signal, with the hope that there exists at least one NM-graph. Note that in our algorithm, we do not need to know which bipartite graph is an NM-graph. We just perform the decoding as if the graph is an NM-graph, even if this may not be true. To see this, suppose the graph G_l is not an NM-graph and contains a multiton. The multiton right node is a superposition of multiple active left nodes, say, x_{n_1} and x_{n_2} , i.e.

$$\mathbf{y}_{l,m} = \begin{bmatrix} |x_{n_1} + x_{n_2}| \\ |2(\cos(n_1\omega)x_{n_1} + \cos(n_2\omega)x_{n_2})| \end{bmatrix} \quad (21)$$

Clearly, performing (20) by treating $\mathbf{y}_{l,m}$ as a singleton yields incorrect location index and magnitude information. Nevertheless, in this case, it is clear that the estimate of $z = |\mathbf{x}|$ based on \mathbf{y}_l , denoted as $\hat{z}^{(l)}$, contains less than K nonzero components. This is an important observation based on which we can differentiate the correct estimate from incorrect estimates. Due to the fact that K is unknown in practice, given the L estimates $\{\hat{z}^{(l)}\}_{l=1}^L$, the final estimate can be chosen to be the one which has the largest number of nonzero entries. Obviously, our proposed algorithm succeeds to recover the support and magnitude of the sparse signal as long as there exists at least one NM-graph. For clarity, our proposed algorithm is summarized in Algorithm 1.

We see that, through the use of multiple bipartite graphs, the proposed SBG-Code circumvents the complicated decoding procedure that is needed by PhaseCode to check whether a right node is a singleton, a mergeable multiton or a resolvable multiton. Although the use of multiple bipartite graphs could bring a higher sample complexity, the simplified decoding procedure can help improve the robustness against measurement errors and noise.

C. Discussions

It should be noted that the cosine function used in (14) to encode the sparse signal can be replaced by a general function. For example, a linear function $f(n) = n/N$ can be employed to encode the sparse signal, in which case the trigonometric modulation matrix \mathbf{T} is expressed as

$$\mathbf{T} = \begin{bmatrix} 1 & 1 & \cdots & 1 \\ 1/N & 2/N & \cdots & 1 \end{bmatrix} \quad (22)$$

Correspondingly, the m th singleton right node can be written as

$$\mathbf{y}_{l,m} = \begin{bmatrix} |x_n| \\ |nx_n/N| \end{bmatrix} \quad (23)$$

and the magnitude and location index of x_n can be readily estimated as

$$\begin{aligned} z_{\hat{n}} &= y_{l,m}^{(1)} \\ \hat{n} &= \frac{Ny_{l,m}^{(2)}}{y_{l,m}^{(1)}} \end{aligned} \quad (24)$$

V. THEORETICAL ANALYSIS FOR SBG-CODE

We now provide theoretical guarantees for our proposed SBG-Code scheme. We first analyze the probability of a bipartite graph being an NM-graph. To simplify our analysis, we assume $r \triangleq N/M$ is an integer. The results are summarized as follows.

A. Main Results

Proposition 1: Suppose we have

$$\mathbf{y}_l = |\mathbf{A}_l \mathbf{x}| \quad (25)$$

where $\mathbf{x} \in \mathbb{C}^N$ is a K -sparse signal, and the location indexes of its nonzero components are chosen uniformly at random. \mathbf{A}_l is defined in (17), in which $\mathbf{H}_l \in \{0, 1\}^{M \times N}$ is a binary code matrix constructed according to a given bipartite graph G_l . Specifically, \mathbf{H}_l (i.e. G_l) is designed such that each column of \mathbf{H}_l has at least one nonzero element, and the m th row of \mathbf{H}_l has r_m nonzero elements. If $M \geq K$, then the probability that all right nodes of G_l are either singletons or nulltons is upper bounded by

$$P(G_l \text{ is an NM-graph}) \leq r^K C_M^K / C_N^K \triangleq \lambda \quad (26)$$

where C_N^K denotes the number of K -combinations from a set with N elements. Also, the inequality (26) becomes an equality if and only if

$$r_1 = \cdots = r_M = r \quad (27)$$

Proof: See Appendix A. ■

From Proposition 1, we know that the probability of a bipartite graph being an NM-graph is maximized when $r_m = r, \forall m$, in which case each column of \mathbf{H}_l has only one nonzero element, and each row of \mathbf{H}_l has exactly r nonzero elements. This result explains why we devise the bipartite graphs $\{G_l\}$ as discussed in Section IV.A. Based on this result,

our proposed phaseless decoding scheme can recover $z = |\mathbf{x}|$ from compressive phaseless measurements with probability given as follows.

Theorem 1: Consider the phaseless decoding problem described in (16), where the measurement matrix $\mathbf{A} \in \mathbb{R}^{2ML \times N}$ is generated according to our proposed sparse encoding scheme. If $M \geq K$, then our proposed algorithm can recover $z = |\mathbf{x}|$ from phaseless measurements (16) with probability exceeding

$$p = 1 - (1 - \lambda)^L \quad (28)$$

where λ is defined in (26).

Proof: See Appendix B. ■

Note that our proposed algorithm requires a total number of $T = 2ML$ phaseless measurements, in which M is the number of right nodes per bipartite graph and L is the number of bipartite graphs. From (26), we see that increasing M helps achieve a higher λ , which in turn leads to a higher recovery probability for our algorithm. On the other hand, increasing L improves the probability that there exists at least one NM-graph among those L bipartite graphs, and thus can also enhance the recovery probability. Therefore, given the total number of measurements T fixed, there is a tradeoff between the choice of M and L . Here we provide an example to illustrate this tradeoff. Suppose $N = 128$, $K = 2$ and $T = 32$. The parameters M and L can be chosen as one of the following cases, and the exact recovery probability of our proposed algorithm can be accordingly calculated:

- $M = 16, L = 1: p = 94.4882\%$
- $M = 8, L = 2: p = 98.6050\%$
- $M = 4, L = 4: p = 99.6450\%$
- $M = 2, L = 8: p = 99.6333\%$

From this example, we see that choosing a moderate value for M and L provides the best performance.

B. Analysis of Sample Complexity

Let $M = \delta K$, where $\delta > 1$ is parameter whose choice will be discussed later. From Theorem 1, we can derive the number of bipartite graphs required for perfectly recovering $|\mathbf{x}|$ with probability exceeding a prescribed threshold p_0 :

$$L \geq \frac{\log(1 - p_0)}{\log(1 - \lambda)} = \frac{\log[(1 - p_0)^{-1}]}{\log[(1 - \lambda)^{-1}]} \quad (29)$$

As a result, the total number of measurements required for exact recovery with probability exceeding p_0 is given by

$$T = 2ML = 2\delta KL \geq \frac{c\delta K}{\log[(1 - \lambda)^{-1}]} \quad (30)$$

where $c \triangleq 2 \log[(1 - p_0)^{-1}] > 0$ is a constant determined by p_0 . Note that λ defined in (26) can be lower bounded by

$$\begin{aligned} \lambda &= \frac{M!}{M^K (M - K)!} \frac{N^K (N - K)!}{N!} \\ &\geq \frac{M!}{M^K (M - K)!} \\ &\geq \frac{(M - K + 1)^K}{M^K} = \left(1 - \frac{1 - K^{-1}}{\delta}\right)^K \triangleq f(K, \delta) \end{aligned} \quad (31)$$

Define

$$h(K, \delta) \triangleq \frac{1}{\log[(1 - f(K, \delta))^{-1}]} \quad (32)$$

The term on the right-hand side of (30) can be upper bounded by

$$\frac{c\delta K}{\log[(1 - \lambda)^{-1}]} \leq c\delta K h(K, \delta) \quad (33)$$

To facilitate analyzing the sample complexity of our proposed algorithm, we choose $\delta = K$, i.e. $M = K^2$, which is a choice usually offering satisfactory performance. In this case, it can be easily proved that the function $f(K, \delta)$ decreases with an increasing K , and

$$\lim_{K \rightarrow +\infty} f(K, \delta) |_{\delta=K} = e^{-1} \quad (34)$$

Therefore $h(K, \delta) |_{\delta=K}$ can be upper bounded by

$$h(K, \delta) |_{\delta=K} \leq \frac{1}{\log[(1 - e^{-1})^{-1}]} \approx 1.51 \quad (35)$$

Combining (33) and (35), we can reach that, when $\delta = K$, the term on the right-hand side of (30) is upper bounded by

$$\frac{c\delta K}{\log[(1 - \lambda)^{-1}]} \leq 1.51cK^2 \quad (36)$$

In other words, if the total number of phaseless measurements T satisfies

$$T \geq 1.51cK^2 \quad (37)$$

then our proposed algorithm can perfectly recover $|\mathbf{x}|$ with probability exceeding p_0 . From (37), we see that the sample complexity for our proposed algorithm is of order $\mathcal{O}(K^2)$, which, surprisingly, is independent of the dimension of the sparse signal, N . Such a result can be well explained because for the typical choice of $\delta = K$, the probability of a bipartite graph being an NM-graph is lower bounded by e^{-1} (cf. (34)) even for an arbitrarily large N . But notice that the irrelevance of the sample complexity to N is achieved by increasing r since we have $r = N/M$ and M is kept fixed as K^2 as N grows. In the beam alignment application, r cannot become arbitrarily large due to the limited number of RF chains.

Although a typical choice of $M = K^2$ is adopted for analyzing the sample complexity, it should not be difficult to reach a similar conclusion for a general choice of M with $M = \mathcal{O}(K^2)$. As a comparison, note that the sample complexity attained by most compressive phase retrieval methods [27], [28] and the AgileLink beam steering scheme [8], [24] is of order $\mathcal{O}(K \log(N))$.

VI. ROBUST SBG-CODE ALGORITHM

The basic idea of our proposed GF-Code algorithm is to divide the N components of \mathbf{x} (i.e. N left nodes) into M disjoint sets, and each set of left nodes is connected to an individual right node. If a right node is a singleton, it means that its corresponding set of left nodes contains only one active left node whose location and magnitude can be easily estimated via (20) or (24), depending on which modulation matrix is used. Such an idea works perfectly for the noiseless

case. Nevertheless, when the measurements are corrupted by noise, a perfect estimate of the magnitude of the active left node is impossible. Besides, the location index of the active left node may be incorrectly estimated as well. In the following, we develop a robust scheme for sparse encoding and phaseless decoding in the presence of noise.

A. Robust Sparse Encoding

To facilitate our following exposition, the trigonometric modulation matrix (14) or (22) is expressed as a general form as

$$\mathbf{T} \triangleq \begin{bmatrix} 1 & 1 & \cdots & 1 \\ t_1 & t_2 & \cdots & t_n \end{bmatrix} \quad (38)$$

where $t_i \neq t_j$ for $i \neq j$, and $t_n > 0, \forall n = 1, \dots, N$. Let $\{m_1^{(l)}, \dots, m_r^{(l)}\}$ denote the set of indices of the left nodes connected to the m th right node of the graph G_l . Note that the index set $\{m_1^{(l)}, \dots, m_r^{(l)}\}$ is determined once the corresponding bipartite graph G_l , i.e. \mathbf{H}_l , is given. Here we assume $r = N/M$ is an integer. The extension to the non-integer case is straightforward, as discussed earlier in Section IV. Also, for simplicity, the superscript l used to denote the index of the bipartite graph is omitted, and in the following, $\{m_1^{(l)}, \dots, m_r^{(l)}\}$ is simplified as $\{m_1, \dots, m_r\}$.

Suppose the m th right node is a singleton and x_{m_i} is the active left node connected to the m th right node, in which $m_i \in \{m_1, \dots, m_r\}$. When noise is present, the measurements corresponding to the m th right node of the graph G_l can be expressed as

$$\mathbf{y}_{l,m} = \begin{bmatrix} |x_{m_i} + w_{l,m}^{(1)}| \\ |t_{m_i} x_{m_i} + w_{l,m}^{(2)}| \end{bmatrix} \triangleq \begin{bmatrix} y_{l,m}^{(1)} \\ y_{l,m}^{(2)} \end{bmatrix} \quad (39)$$

where $w_{l,m}^{(1)}$ and $w_{l,m}^{(2)}$ denote the observation noise added to the first and the second entry of the m th right node, respectively. In this case, the location index of the active left node can be estimated as

$$\hat{m}_i = \underset{m_i \in \{m_1, \dots, m_r\}}{\operatorname{arg\,min}} \left| t_{m_i} - \frac{y_{l,m}^{(2)}}{y_{l,m}^{(1)}} \right| \quad (40)$$

The problem lies in that, if the index set $\{m_1, \dots, m_r\}$ contains an element m_j such that t_{m_j} is close to t_{m_i} , then it is likely that the location index of the active left node is misidentified as m_j since when noise is present, we may have

$$\left| t_{m_i} - \frac{y_{l,m}^{(2)}}{y_{l,m}^{(1)}} \right| > \left| t_{m_j} - \frac{y_{l,m}^{(2)}}{y_{l,m}^{(1)}} \right| \quad (41)$$

To improve robustness against noise, it is clear that the absolute difference $|t_{m_i} - t_{m_j}|$ should be as large as possible for any pair of indices $\{m_i, m_j\}$ chosen from the set $\{m_1, \dots, m_r\}$.

Inspired by this insight, we propose to use an individual modulation matrix for each bipartite graph. Specifically, the modulation matrix for each bipartite graph is a column-permuted version of the original modulation matrix, i.e.

$$\mathbf{T}_l = \mathbf{T} \mathbf{P}_l \quad \forall l \quad (42)$$

where \mathbf{T}_l denotes the modulation matrix for graph G_l , and \mathbf{P}_l is a permutation matrix to be devised. Write

$$\mathbf{T}_l \triangleq \begin{bmatrix} 1 & 1 & \cdots & 1 \\ t_1^{(l)} & t_2^{(l)} & \cdots & t_N^{(l)} \end{bmatrix} \quad (43)$$

Following a similar deduction, the location index of the active left node associated with the m th right node can be estimated as

$$\hat{m}_i = \arg \min_{m_i \in \{m_1, \dots, m_r\}} \left| t_{m_i}^{(l)} - \frac{y_{l,m}^{(2)}}{y_{l,m}^{(1)}} \right| \quad (44)$$

Therefore, if the permutation matrix \mathbf{P}_l is devised such that for each right node m , the elements in the corresponding set $\{t_{m_1}^{(l)}, \dots, t_{m_r}^{(l)}\}$ are sufficiently separated, then the robustness against noise can be improved. To put it in a mathematical way, define the pairwise distance associated with the m th right node as

$$d_m^{(l)} \triangleq \min_{1 \leq i < j \leq r} |t_{m_i}^{(l)} - t_{m_j}^{(l)}| \quad (45)$$

Then the design of \mathbf{P}_l can be formulated as a Max-Min problem whose objective is to maximize the minimum pairwise distance among the pairwise distances associated with M right nodes, i.e.

$$\max_{\mathbf{P}_l} \min_m d_m^{(l)} \quad (46)$$

Such an optimization can be solved by searching for all possible permutation matrices. Note that it is more advantageous to use an individual permutation matrix for each graph than using a common permutation matrix for all graphs because employing an individual permutation matrix for each graph can help achieve a larger minimum pairwise distance.

B. Robust Phaseless Decoding

We next devise a robust decoding scheme to estimate $\mathbf{z} = |\mathbf{x}|$ from noisy measurements \mathbf{y} . In the noisy case, the measurements \mathbf{y} are written as

$$\mathbf{y} = |\mathbf{A}\mathbf{x} + \mathbf{w}| \quad (47)$$

where the measurement matrix \mathbf{A} is expressed as

$$\mathbf{A} \triangleq \begin{bmatrix} \mathbf{A}_1 \\ \mathbf{A}_2 \\ \vdots \\ \mathbf{A}_L \end{bmatrix} \triangleq \begin{bmatrix} \mathbf{H}_1 \odot \mathbf{T}_1 \\ \mathbf{H}_2 \odot \mathbf{T}_2 \\ \vdots \\ \mathbf{H}_L \odot \mathbf{T}_L \end{bmatrix} \quad (48)$$

and the modulation matrix \mathbf{T}_l for graph G_l is given by (42). The measurements associated with the bipartite graph G_l are given by

$$\mathbf{y}_l \triangleq |\mathbf{A}_l \mathbf{x} + \mathbf{w}_l| \quad (49)$$

and the measurements, $\mathbf{y}_{l,m} \in \mathbb{R}^2$, corresponding to the m th right node of G_l are expressed as

$$\mathbf{y}_{l,m} = |(\mathbf{H}_l[m, :] \odot \mathbf{T}_l) \mathbf{x} + \mathbf{w}_{l,m}| \quad \forall m = 1, \dots, M \quad (50)$$

where $\mathbf{w}_{l,m}$ denotes the noise added to the m th right node of G_l . Due to the presence of noise, we usually have $\mathbf{y}_{l,m} \neq$

$\mathbf{0}$ even if the m th right node is a nullton. Hence we first need to decide whether a right node of G_l is a nullton or not. Such a problem can be formulated as a binary hypothesis test problem:

$$\begin{aligned} H_0 : y_{l,m}^{(1)} &= |w_{l,m}^{(1)}| \\ H_1 : y_{l,m}^{(1)} &= \left| \sum_{m_i \in S} x_{m_i} + w_{l,m}^{(1)} \right| \end{aligned} \quad (51)$$

where $w_{l,m}^{(1)}$ is the additive complex Gaussian noise with zero mean and variance σ^2 , and S denotes the set of indices of those active left nodes that are connected to the m th right node. A simple energy detector can be used to perform the detection:

$$y_{l,m}^{(1)} \underset{H_0}{\overset{H_1}{\gtrless}} \epsilon \quad (52)$$

It is clear that $y_{l,m}^{(1)}$ under H_0 follows a Rayleigh distribution. Given a prescribed false alarm probability, the threshold $\epsilon > 0$ can be easily determined from the distribution of $y_{l,m}^{(1)}$ under H_0 . Such an energy detector is able to yield satisfactory detection performance for a moderate and high signal-to-noise ratio.

To proceed with our decoding scheme, we assume all nullton right nodes of G_l are correctly identified. In this case, we are able to determine whether G_l is an NM-graph or not. Specifically, if G_l is an NM-graph, then it contains $M - K$ nullton right nodes; otherwise the number of nullton right nodes is greater than $M - K$. Although the number of active left nodes, K , is unknown *a priori*, those graphs which have the smallest number of nullton right nodes can be considered as NM-graphs and K can be simply estimated as

$$\hat{K} = M - J \quad (53)$$

where J denotes the smallest number of nullton right nodes among all graphs.

We now perform decoding on those NM-graphs. Suppose G_l is an NM-graph and its m th right node is a singleton. Also, x_{m_i} is the active left node connected to the m th right node. From the discussion in the previous subsection, it is clear that the magnitude and location index of this active left node can be estimated as

$$\begin{aligned} z_{\hat{m}_i} &= y_{l,m}^{(1)} \\ \hat{m}_i &= \arg \min_{m_i \in \{m_1, \dots, m_r\}} \left| t_{m_i}^{(l)} - \frac{y_{l,m}^{(2)}}{y_{l,m}^{(1)}} \right| \end{aligned} \quad (54)$$

where $\{m_1, \dots, m_r\}$ denotes the set of indices of those left nodes connected to the m th right node. After performing (54) for all singleton right nodes, we are able to obtain an estimate of $\mathbf{z} = |\mathbf{x}|$. Let $\hat{\mathbf{z}}^{(l)}$ denote an estimate of \mathbf{z} obtained from the measurements associated with G_l . Since we may have more than one NM-graphs, we are able to collect multiple estimates of \mathbf{z} . The problem lies in, due to the existence of noise, these multiple estimates, denoted as $\{\hat{\mathbf{z}}^{(1)}, \dots, \hat{\mathbf{z}}^{(L)}\}$, are not exactly the same. In the following, we propose a set-intersection scheme to combine these multiple estimates into a more accurate estimate.

To better illustrate our idea, suppose there are two NM-graphs, say G_i and G_j , and x_n is the only active left node in \mathbf{x} . Recall that for each bipartite graph, the N left nodes are divided into M disjoint sets, with each set of left nodes connected to an individual right node. Let $S_n^{(i)}$ denote the set of left nodes to which x_n belongs in graph G_i , and $S_n^{(j)}$ denote the set of left nodes to which x_n belongs in graph G_j . Suppose the singleton right nodes in both G_i and G_j are correctly identified. Then we know that x_n belongs to both $S_n^{(i)}$ and $S_n^{(j)}$. If the intersection of the two sets $S_n^{(i)}$ and $S_n^{(j)}$, $S_n^{(i)} \cap S_n^{(j)}$, contains only one element, then it must be x_n and the location of x_n can be uniquely determined. Such an idea can be easily extended to the scenario where there are more than two NM-graphs, and for such a case, the set-intersection scheme is more likely to succeed because the more sets are used, the higher the probability of the intersection of these sets containing only one element.

There, however, is a problem for the general case where \mathbf{x} contains multiple nonzero components (i.e. multiple active left nodes). In this case, we have no idea which set of left nodes a certain active node belongs to for each NM-graph. As a result, it is impossible to determine which sets should be put together to perform the intersection operation. To overcome this difficulty, we note that the magnitudes of those active left nodes are generally different. Hence the estimated magnitude can be used to identify a certain active left node. Without loss of generality, let x_1, \dots, x_K denote the nonzero components of \mathbf{x} in decreasing order in terms of magnitude, i.e. $|x_1| > \dots > |x_K| > 0$. For each NM-graph, say graph G_i , we can obtain an estimate of $|\mathbf{x}|$, denoted as $\mathbf{z}^{(i)}$. Specifically, let $\hat{z}_{i_1} > \dots > \hat{z}_{i_K} > 0$ represent the nonzero components of $\hat{\mathbf{z}}^{(i)}$, then the k th largest element \hat{z}_{i_k} can be regarded as an estimate of $|x_k|$. For each NM-graph, say G_i , the set of left nodes containing x_k can therefore be determined as the set of left nodes containing \hat{z}_{i_k} . A set intersection operation can then be performed to yield the final estimate of the location index of x_k . On the other hand, the magnitude of the k th largest component of \mathbf{x} can be estimated as the average of all estimates, i.e.

$$|\hat{x}_k| = \frac{1}{I} \sum_{i=1}^I \hat{z}_{i_k} \quad (55)$$

Note that if the intersection of the sets contains more than one element, then we randomly pick up an element in the intersection set as the estimate of the location index of x_k . In addition, in case the intersection is an empty set, which is possible due to the incorrect association between $\{x_1, \dots, x_K\}$ and $\{\hat{z}_{i_1}, \dots, \hat{z}_{i_K}\}$, we randomly select an estimate from $\{\hat{\mathbf{z}}^{(1)}, \dots, \hat{\mathbf{z}}^{(I)}\}$ as the final estimate. For clarity, our proposed robust SBG-Code algorithm is summarized in Algorithm 2. We see the proposed decoding algorithm involves very simple addition and multiplication calculations, and thus is amiable for practical implementation.

VII. EXTENSION TO ANTENNA ARRAY RECEIVER

In Section II, we assume the receiver employs an omnidirectional antenna that receives in all directions. In this

Algorithm 2 Robust SBG-Code Algorithm

Given $\mathbf{A}_l = \mathbf{H}_l \odot \tilde{\mathbf{T}}_l$ and \mathbf{y}_l for each bipartite graph G_l , $l = 1, \dots, L$
for $l = 1, \dots, L$ **do**
 Decide whether a right node of G_l is a nullton or not via the energy detector (52). Count the number of nulltons of G_l .
end for
Find graphs that have the smallest number of nulltons and consider them as NM-graphs
for $l = 1, \dots, L$ **do**
 if G_l is an NM-graph **then**
 for $m = 1, \dots, M$ **do**
 if $y_{l,m}^{(1)} > \epsilon$ **then**
 Assume the m th right node is a singleton
 Estimate the magnitude and the location index of the active left node connected to the m th right node via (54)
 end if
 end for
 Obtain the estimate $\hat{\mathbf{z}}^{(l)}$
 end if
end for
Given multiple estimates $\{\hat{\mathbf{z}}^{(l)}\}_{l=1}^I$
if $I = 1$ **then**
 Choose $\hat{\mathbf{z}}^{(1)}$ as the final estimate
else
 Resort to the set-intersection-check scheme to obtain a final estimate
end if

section, we extend to the case where both the transmitter and the receiver have antenna arrays for beam alignment. With a slight abuse of notation, we let N_t and N_r denote the number of antennas at the transmitter and the receiver, respectively. The mmWave channel is characterized by a geometric channel model

$$\mathbf{G} = \sum_{p=1}^P \alpha_p \mathbf{a}_r(\theta_p) \mathbf{a}_t^H(\phi_p) \quad (56)$$

where P is the number of paths, α_p is the complex gain associated with the p th path, $\theta_p \in [0, 2\pi]$ and $\phi_p \in [0, 2\pi]$ are the associated azimuth angle of arrival (AoA) and angle of departure (AoD), respectively, and $\mathbf{a}_r \in \mathbb{C}^{N_r}$ ($\mathbf{a}_t \in \mathbb{C}^{N_t}$) denotes the receiver (transmitter) array response vector. We assume that the uniform linear array is used at both the transmitter and receiver. Since there are only a few paths between the transmitter and the receiver, the channel matrix in the beam space domain has a sparse representation

$$\mathbf{G} = \mathbf{D}_r \tilde{\mathbf{G}} \mathbf{D}_t^H \quad (57)$$

where $\mathbf{D}_r \in \mathbb{C}^{N_r \times N_r}$ and $\mathbf{D}_t \in \mathbb{C}^{N_t \times N_t}$ are the DFT matrices, and $\tilde{\mathbf{G}} \in \mathbb{C}^{N_r \times N_t}$ is a sparse matrix. Suppose the transmitter sends a constant signal $s(t) = 1$ to the receiver. The phaseless measurement received at the t th time instant

can be expressed as

$$\begin{aligned} y(t) &= |\mathbf{c}^H(t)\mathbf{G}\mathbf{b}(t)s(t) + w(t)| \\ &= |\mathbf{c}^H(t)\mathbf{D}_r\tilde{\mathbf{G}}\mathbf{D}_t^H\mathbf{b}(t) + w(t)| \end{aligned} \quad (58)$$

where $\mathbf{c}(t)$ denotes the combining vector used at the receiver. To perform beam alignment, we can let the receiver steer its beam to a fixed direction over a period of time (or multiple beams towards different directions if multiple RF chains at the receiver are available), and let the transmitter send the codewords devised according to our proposed sparse encoding scheme. Specifically, the receiver uses a certain column of \mathbf{D}_r as its combining vector, i.e. $\mathbf{c}(t) = \mathbf{D}_r[:, i]$, over a period of time, say $t = 1, \dots, T$. The beamforming vector employed by the transmitter is the same as discussed in Section II, i.e. $\mathbf{b}(t) = \mathbf{D}_t\mathbf{S}(t)\mathbf{f}_{\text{BB}}(t) \triangleq \mathbf{D}_t\mathbf{a}(t)$. Thus we have

$$y(t) = |\mathbf{a}^H(t)\bar{\mathbf{g}}_i + w^*(t)| \quad t = 1, \dots, T \quad (59)$$

where $\bar{\mathbf{g}}_i$ denotes the i th column of $\tilde{\mathbf{G}}^H$. We see that the problem is now converted to the sparse encoding and phaseless decoding problem discussed in this paper, and our proposed scheme can be used to recover $|\bar{\mathbf{g}}_i|$. After the receiver has scanned all possible N_r beam directions, we are able to obtain the full knowledge of $|\tilde{\mathbf{G}}|$, based on which the best beamformer-combiner pair can be obtained. Such a beam alignment scheme has a sample complexity of $\mathcal{O}(N_r\bar{K}^2/R_r)$, where R_r represents the number of RF chains at the receiver, and $\bar{K} \triangleq \max\{K_1, \dots, K_{N_r}\}$, with K_i denoting the number of nonzero entries in the i th column of $\tilde{\mathbf{G}}^H$, i.e. $\bar{\mathbf{g}}_i$. Clearly, \bar{K} is much smaller than the total number of paths P .

VIII. SIMULATION RESULTS

We now present simulation results to illustrate the performance of our proposed SBG-Code algorithm. In our simulations, the transmitter employs a ULA with N antennas and R RF chains, while the receiver uses an omni-directional antenna. The distance between neighboring antenna elements is assumed to be $d = \lambda/2$. The mmWave channel \mathbf{h} is assumed to have a form of (4) with K paths. The nonzero components of \mathbf{x} are assumed to be random variables following a circularly symmetric complex Gaussian distribution $\mathcal{CN}(0, 1)$, and the locations of nonzero entries of \mathbf{x} are uniformly chosen at random. All the results are averaged over 10^4 independent runs. In each run, \mathbf{x} (i.e. \mathbf{h}) is randomly generated. The linear function $f(n) = n/N$ is employed to encode the sparse signal, i.e. the trigonometric modulation matrix is given by (22), and the estimator (24) is used to estimate \mathbf{z} in the noiseless case.

We first examine the estimation performance of our proposed algorithm in the noiseless case. The performance is evaluated via the success rate, which is computed as the ratio of the number of successful trials to the total number of independent runs. A trial is considered successful if $\|\hat{\mathbf{z}} - \mathbf{z}\|_2^2 / \|\mathbf{z}\|_2^2 < 10^{-8}$, where $\hat{\mathbf{z}}$ denotes the estimate of \mathbf{z} . Fig. 3(a) depicts the success rates as a function of the number of measurements $T = 2ML$, where the number of antennas is set to $N = 128$, the number of RF chains is set to $R = 8$, and the number of right nodes in each bipartite graph is set to $M = 16$. In the figure, solid lines represent the theoretical

performance given in (28), while the circle marks represent the performance obtained via the Monte Carlo experiments. From Fig. 3, we see that our theoretical result matches the empirical result very well. Also, when the number of paths K is small, our proposed scheme can perfectly recover the AoA and the attenuation (in magnitude) of each path with a decent probability even using a small number of measurements, say $T = 32$, thus achieving a substantial overhead reduction for beam alignment. Fig. 3(b) plots the success rates as a function of the dimension of the sparse signal N , where we set $T = 64$, $R = 8$, and $M = 16$. From Fig. 3(b), we observe that the success rate of our proposed algorithm remains almost unaltered as N grows. This result corroborates our theoretical claim that our proposed algorithm has a sample complexity independent of N . It is also interesting to examine the impact of the choice of the number of right nodes per bipartite graph, M , on the performance of our proposed algorithm, given the total number of measurements T fixed. Fig. 3(c) plots the success rates as a function of M , where we set $T = 64$ and $N = 128$. Note that since the parameter M must be chosen such that $R \geq \text{floor}(N/M)$, the number of required RF chains changes as M varies. From Fig. 3(c), we see that the best performance is achieved when $M \approx K^2$.

Next, we illustrate the estimation performance of our proposed algorithm in the noisy case. We compare our method with the robust PhaseCode algorithm. As mentioned earlier in our paper, PhaseCode uses a single randomly generated bipartite graph to encode the sparse signal. The resulting measurement matrix \mathbf{A} may not satisfy constraint C1. To fulfil the potential of PhaseCode, we allow the constraint C1 to be violated by PhaseCode. For our proposed method, the prescribed false alarm probability used to determine the threshold in the energy detector (52) is set to $e^{-9/2} \approx 0.011$, thus the threshold is given by $\epsilon = 3\sigma$. For a fair comparison, the beamforming vector $\mathbf{b}(t)$ (cf. (6)) used in both schemes is normalized to unit norm. The performance is evaluated via the normalized mean squared error (NMSE) calculated as

$$\text{NMSE} = E \left[\frac{\|\hat{\mathbf{z}} - \mathbf{z}\|_2^2}{\|\mathbf{z}\|_2^2} \right] \quad (60)$$

Note that PhaseCode is able to retrieve the complete information of \mathbf{x} . But the accuracy of the estimate of $\mathbf{z} = |\mathbf{x}|$ is of most concern for beam alignment. Fig. 4(a) shows the NMSEs of respective schemes as a function of T , where we set $N = 128$, $M = 16$, and the SNR is set to 20dB. Here the SNR is defined as

$$\text{SNR} = 10 \log(\|\mathbf{h}\|_2^2 / (N\sigma^2)) \quad (61)$$

From Fig. 4(a), we see that our proposed method outperforms the robust PhaseCode method by a big margin for difference choices of K . The performance improvement is primarily due to the fact that our proposed method circumvents the complicated decoding procedure that is needed for PhaseCode and thus gains substantially improved robustness against noise. Fig. 4(b) depicts the NMSEs of respective schemes as a function of SNR, where we set $T = 64$ and $M = 16$. It can be observed that our proposed method attains a decent

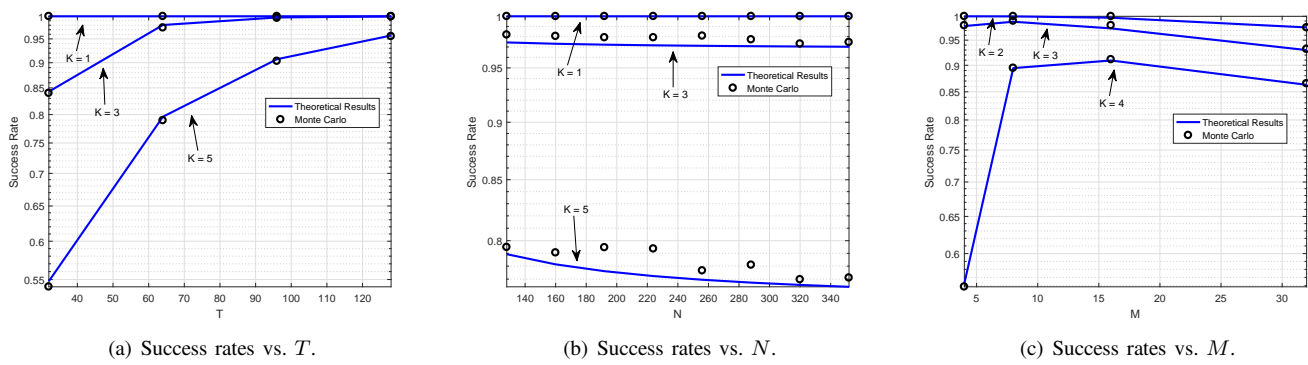


Fig. 3. Success rates of our proposed method vs. T , N , and M in the noiseless case.

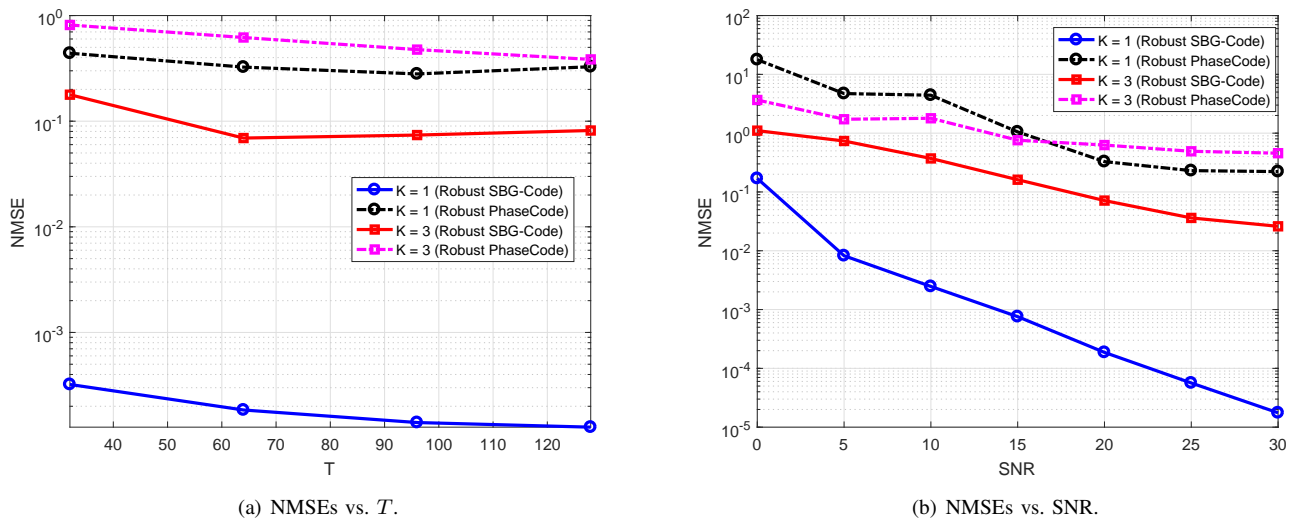


Fig. 4. NMSEs of respective algorithms vs. T and SNR.

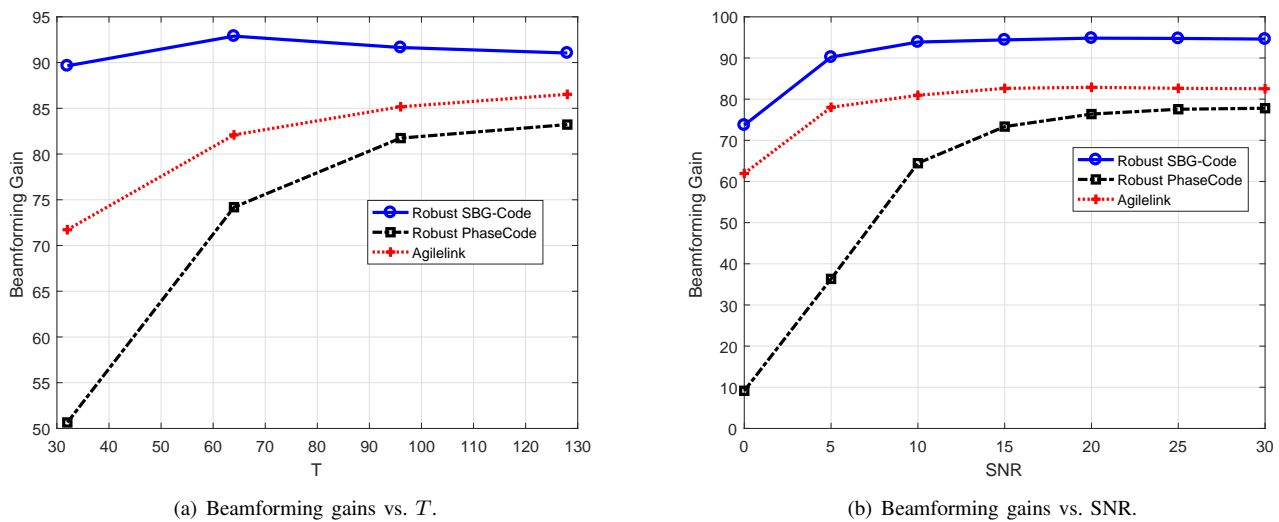


Fig. 5. Beamforming gains of respective algorithms vs. T and SNR.

accuracy even in the low and moderate SNR regimes, whereas the robust PhaseCode fails in this case.

Lastly, we compare our proposed algorithm with the Agile-

Link [8], a beam steering scheme which also relies on the magnitude information of measurements for recovery of signal directions. It should be noted that Alige-Link only recovers

signal directions, but not z . The beamforming gain defined below is used as a metric to evaluate the performance of respective schemes

$$G_{\text{BF}} = E \left[N |\mathbf{a}_t^H(\hat{\theta}_{\text{opt}}) \mathbf{h}|^2 / \|\mathbf{h}\|_2^2 \right] \quad (62)$$

in which $\hat{\theta}_{\text{opt}}$ denotes the estimated direction of path that delivers the maximum energy. For the Agile-Link, $\hat{\theta}_{\text{opt}}$ is estimated as the direction with the highest probability. Fig. 5(a) depicts the beamforming gains of respective algorithms as a function of T , where we set $N = 128$, $K = 2$, $M = 16$, and SNR = 15dB. Again, for a fair comparison, the beamforming vector $\mathbf{b}(t)$ used in these schemes is normalized to unit norm. We see that our proposed method yields a higher beamforming gain than the Agile-Link and the PhaseCode, and the performance gap is particularly pronounced when the number of measurements T is small. This result suggests that our proposed method can help find a better beam alignment. Fig. 5(b) plots the beamforming gains of respective algorithms as a function of SNR, where we set $T = 64$, $K = 2$, and $M = 32$, from which we can see that our proposed method even renders a decent beamforming gain in the low SNR regime.

IX. CONCLUSIONS

The problem of mmWave beam alignment was examined in this paper. By exploiting the sparse scattering nature of mmWave channels, we showed that the problem of beam alignment can be formulated as a sparse encoding and phaseless decoding problem. A SBG-Code method was developed to encode the sparse signal and retrieve the support and magnitude information of the sparse signal from compressive phaseless measurements. Our analysis revealed that the proposed method can provably recover the sparse signal with a pre-specified probability from $\mathcal{O}(K^2)$ phaseless measurements. Simulation results showed that the proposed scheme renders a reliable beam alignment even in a low or moderate SNR regime with very few measurements, and presents a clear advantage over existing mmWave beam alignment algorithms.

APPENDIX A PROOF OF PROPOSITION 1

Before preceding, we first show that the probability that all right nodes of G_l are either singletons or nulltons is maximized when each column of \mathbf{H}_l has only one nonzero element, i.e. each left node is connected to only one right node. Such a fact can be easily verified via an edge-deletion operation performed on G_l . Specifically, for each left node of G_l , if it has more than one edge, that is, it is connected to more than one right node, then we reserve only one edge and delete all the other edges. It is clear that after the edge-deletion operation, the number of singletons and nulltons of G_l either keeps increased or unchanged. Therefore, the probability that all right nodes of G_l are either singletons or nulltons is maximized when each column of \mathbf{H}_l has only one nonzero element. Note than in this case, we have

$$\sum_{m=1}^M r_m = rM = N \quad (63)$$

We now calculate the probability that G_l is an NM-graph when each left node is connected to only one right node. More precisely, we divide N left nodes into M disjoint sets, where the m th set consisting of r_m left nodes is connected to the m th right node. There are K active left nodes in total. We need to calculate the probability that each set of left nodes, denoted as S_m , contains at most one active left node. Define

$$\mathcal{M} \triangleq \{1, \dots, M\} \quad (64)$$

Let $\mathcal{K} \triangleq \{i_1, \dots, i_K\}$ be a subset of \mathcal{M} consisting of K elements, and $\{i_{K+1}, \dots, i_M\} = \mathcal{M} - \mathcal{K}$ be the difference set between \mathcal{M} and \mathcal{K} . It can be easily verified that the number of ways of dividing N left nodes into M disjoint sets such that each set $S_m, m \in \mathcal{K}$, contains only one active left node is given as

$$\begin{aligned} & K! C_{N-K}^{r_{i_1}-1} C_{N-R_1-K+1}^{r_{i_2}-1} \cdots C_{N-R_{K-1}-1}^{r_{i_K}-1} C_{N-R_K}^{r_{i_{K+1}}} \cdots C_{N-R_{M-1}}^{r_{i_M}} \\ &= \frac{K!(N-K)!}{\prod_{t=1}^K (r_{i_t} - 1)! \prod_{t=K+1}^M r_{i_t}!} \end{aligned} \quad (65)$$

where $R_n \triangleq \sum_{t=1}^n r_{i_t}$. Thus, the number of ways of dividing N left nodes into M disjoint sets such that each set contains at most one active left node is given by

$$n_1 \triangleq \sum_{\{i_1, \dots, i_K\} \subseteq \mathcal{M}} \frac{K!(N-K)!}{\prod_{t=1}^K (r_{i_t} - 1)! \prod_{t=K+1}^M r_{i_t}!} \quad (66)$$

On the other hand, the total number of ways of assigning N left nodes to M disjoint sets is given as

$$n_2 \triangleq C_N^{r_1} C_{N-r_1}^{r_2} \cdots C_{N-\sum_{i=1}^{M-1} r_i}^{r_M} = \frac{N!}{\prod_{i=1}^M r_i!} \quad (67)$$

Therefore the probability that G_l is an NM graph can be calculated as

$$P(G_l \text{ is an NM-graph}) = \frac{n_1}{n_2} = \frac{\eta(K)}{C_N^K} \quad (68)$$

where

$$\eta(K) \triangleq \sum_{\{i_1, \dots, i_K\} \subseteq \mathcal{M}} \left(\prod_{t=1}^K r_{i_t} \right) \quad (69)$$

Next, we prove

$$\eta(K) \leq r^K C_M^K \quad (70)$$

holds for all $1 \leq K \leq M$ when $\sum_{i=1}^M r_i = rM$. The inequality (70) is proved by mathematical induction. First, we prove the base case: $K = 1$. It is easy to verify that

$$\eta(1) = \sum_{i=1}^M r_i = rM = r C_M^1 \quad (71)$$

We then proceed to the inductive step. Suppose the following inequality holds for $K' - 1$

$$\eta(K' - 1) \leq r^{K'-1} C_M^{K'-1} \quad (72)$$

We need to prove

$$\eta(K') \leq r^{K'} C_M^{K'} \quad (73)$$

To this goal, we multiply both sides of (72) by $\sum_{i=1}^M r_i$, which yields

$$\begin{aligned} \eta(K' - 1) \left(\sum_{i=1}^M r_i \right) &\leq r^{K'-1} C_M^{K'-1} M r \\ &= M r^{K'} C_M^{K'-1} \end{aligned} \quad (74)$$

The left-hand side of (74) can be further written as

$$\begin{aligned} &\eta(K' - 1) \left(\sum_{i=1}^M r_i \right) \\ &= \sum_{i=1}^M \sum_{\{i_1, \dots, i_{K'-2}\} \subseteq \mathcal{M} - \{i\}} r_i^2 r_{i_1} \cdots r_{i_{K'-2}} + K' \eta(K') \\ &= \frac{1}{M - K' + 1} \sum_{\{i_1, \dots, i_{K'}\} \subseteq \mathcal{M}} \left(\prod_{t=1}^{K'} r_{i_t} \sum_{\substack{j, k \in \{1, \dots, K'\} \\ j \neq k}} \frac{r_{i_k}}{r_{i_j}} \right) \\ &\quad + K' \eta(K') \end{aligned} \quad (75)$$

For any $\{i_1, \dots, i_{K'}\} \subseteq \mathcal{M}$, using the inequality of arithmetic and geometric means (also referred to as the AM-GM inequality), we have

$$\begin{aligned} \sum_{\substack{j, k \in \{1, \dots, K'\} \\ j \neq k}} \frac{r_{i_k}}{r_{i_j}} &\geq K'(K' - 1) \left(\prod_{\substack{j, k \in \{1, \dots, K'\} \\ j \neq k}} \frac{r_{i_k}}{r_{i_j}} \right)^{\frac{1}{K'(K'-1)}} \\ &= K'(K' - 1) \end{aligned} \quad (76)$$

in which the inequality becomes an equality if and only if $r_{i_1} = \cdots = r_{i_{K'}}$. Hence, we have

$$\sum_{\{i_1, \dots, i_{K'}\} \subseteq \mathcal{M}} \left(\prod_{t=1}^{K'} r_{i_t} \sum_{\substack{j, t \in \{1, \dots, K'\} \\ j \neq t}} \frac{r_{i_t}}{r_{i_j}} \right) \geq K'(K' - 1) \eta(K') \quad (77)$$

in which the inequality (77) becomes equality if and only if $r_1 = \cdots = r_M = r$. Combining (74), (75) and (77), we arrive at

$$\begin{aligned} M r^{K'} C_M^{K'-1} &\geq \eta(K' - 1) \left(\sum_{i=1}^M r_i \right) \\ &\geq \left(\frac{K'(K' - 1)}{M - K' + 1} + K' \right) \eta(K') = \frac{M K'}{M - K' + 1} \eta(K') \end{aligned} \quad (78)$$

From (78), we have

$$\eta(K') \leq \frac{M - K' + 1}{M K'} M r^{K'} C_M^{K'-1} = r^{K'} C_M^{K'-1} \quad (79)$$

Thus the inductive step is proved. This completes our proof.

APPENDIX B PROOF OF THEOREM 1

According to our proposed algorithm, we see that the support and magnitude information of \mathbf{x} can be perfectly

recovered when there is at least one NM-graph in all bipartite graphs $\{G_l\}_{l=1}^L$. Therefore, the probability that our proposed algorithm succeeds to recover the support and magnitude information of \mathbf{x} equals the probability that there is at least one NM-graph in $\{G_l\}_{l=1}^L$, which is equivalent to

$$p = 1 - (1 - P(G_l \text{ is an NM-graph}))^L = 1 - (1 - \lambda)^L \quad (80)$$

REFERENCES

- [1] T. S. Rappaport, J. N. Murdock, and F. Gutierrez, "State of the art in 60-GHz integrated circuits and systems for wireless communications," *Proc. IEEE*, vol. 99, no. 8, pp. 1390–1436, Aug. 2011.
- [2] S. Rangan, T. S. Rappaport, and E. Erkip, "Millimeter-wave cellular wireless networks: potentials and challenges," *Proc. IEEE*, vol. 102, no. 3, pp. 366–385, March 2014.
- [3] S. Chen and J. Zhao, "The requirements, challenges, and technologies for 5G of terrestrial mobile telecommunication," *IEEE Commun. Mag.*, vol. 52, no. 5, pp. 36–43, May 2014.
- [4] S. Chen, S. Sun, Q. Gao, and X. Su, "Adaptive beamforming in TDD-based mobile communication systems: State of the art and 5G research directions," *IEEE Wireless Commun.*, vol. 23, no. 6, pp. 81–87, Dec. 2016.
- [5] A. L. Swindlehurst, E. Ayanoglu, P. Heydari, and F. Capolino, "Millimeter-wave massive MIMO: the next wireless revolution?" *IEEE Commun. Mag.*, vol. 52, no. 9, pp. 56–62, September 2014.
- [6] A. Alkhateeb, J. Mo, N. Gonzalez-Prelcic, and R. Heath, "MIMO precoding and combining solutions for millimeter-wave systems," *IEEE Commun. Mag.*, vol. 52, no. 12, pp. 122–131, December 2014.
- [7] C. Liu, M. Li, S. V. Hanly, P. Whiting, and I. B. Collings, "Millimeter-Wave small cells: Base station discovery, beam alignment, and system design challenges," *IEEE Wireless Communications*, vol. 25, no. 4, pp. 40–46, August 2018.
- [8] O. Abari, H. Hassanieh, M. Rodriguez, and D. Katabi, "Millimeter wave communications: From point-to-point links to agile network connections," in *Proc. 15th ACM Workshop on Hot Topics in Networks*, Atlanta, Georgia, USA, November 9-10 2016, pp. 169–175.
- [9] J. Song, J. Choi, S. G. Larew, D. J. Love, T. A. Thomas, and A. A. Ghosh, "Adaptive millimeter wave beam alignment for dual-polarized MIMO systems," *IEEE Transactions on Wireless Communications*, vol. 14, no. 11, pp. 6283–6296, Nov. 2015.
- [10] S. Hur, T. Kim, D. J. Love, J. V. Krogmeier, T. A. Thomas, and A. Ghosh, "Millimeter wave beamforming for wireless backhaul and access in small cell networks," *IEEE Trans. Commun.*, vol. 61, no. 10, pp. 4391–4403, October 2013.
- [11] A. Alkhateeb, O. E. Ayach, G. Leus, and R. Heath, "Channel estimation and hybrid precoding for millimeter wave cellular systems," *IEEE J. Sel. Topics Signal Process.*, vol. 8, no. 5, pp. 831–846, October 2014.
- [12] S. Noh, M. D. Zoltowski, and D. J. Love, "Multi-Resolution codebook and adaptive beamforming sequence design for millimeter wave beam alignment," *IEEE Transactions on Wireless Communications*, vol. 16, no. 9, pp. 5689–5701, Sept. 2017.
- [13] M. Hussain and N. Michelusi, "Energy efficient beam-alignment in millimeter wave networks," in *2017 51st Asilomar Conference on Signals, Systems, and Computers*, Pacific Grove, CA, USA, Oct. 29–Nov. 1 2017, pp. 1219–1223.
- [14] A. Alkhateeb, G. Leus, and R. Heath, "Compressed sensing based multi-user millimeter wave systems: How many measurements are needed?" in *Proc. 40th IEEE Inter. Conf. on Acoust., Speech and Signal Process. (ICASSP)*, Brisbane, Australia, April 19–24 2015, pp. 2909–2913.
- [15] P. Schniter and A. Sayeed, "Channel estimation and precoder design for millimeter-wave communications: The sparse way," in *Proc. 48th Asilomar Conf. Signals, Syst. Comput.*, Pacific Grove, California, USA, November 2–5 2014, pp. 273–277.
- [16] T. Kim and D. J. Love, "Virtual AoA and AoD estimation for sparse millimeter wave MIMO channels," in *Proc. 16th IEEE Inter. Workshop on Signal Process. Advances in Wireless Commun. (SPAWC)*, Stockholm, Sweden, June 28 - July 1 2015, pp. 146–150.
- [17] B. Gao, C. Zhang, D. Jin, and L. Zeng, "Compressed SNR-and-channel estimation for beam tracking in 60-GHz WLAN," *China Communications*, vol. 12, no. 6, pp. 46–58, Dec. 2015.
- [18] Z. Marzi, D. Ramasamy, and U. Madhow, "Compressive channel estimation and tracking for large arrays in mm-Wave picocells," *IEEE J. Sel. Topics Signal Process.*, vol. 10, no. 3, pp. 514–527, April 2016.

- [19] Z. Gao, L. Dai, Z. Wang, and S. Chen, "Spatially common sparsity based adaptive channel estimation and feedback for FDD massive MIMO," *IEEE Trans. Signal Process.*, vol. 63, no. 23, pp. 6169–6183, December 2015.
- [20] X. Gao, L. Dai, and A. M. Sayeed, "Low RF-complexity technologies for 5G millimeter-wave MIMO systems with large antenna arrays," *available at arXiv:1607.04559*, 2016.
- [21] Z. Zhou, J. Fang, L. Yang, H. Li, Z. Chen, and S. Li, "Channel estimation for millimeter-wave multiuser MIMO systems via PARAFAC decomposition," *IEEE Trans. Wireless Commun.*, vol. 15, no. 11, pp. 7501–7516, November 2016.
- [22] Z. Zhou, J. Fang, L. Yang, H. Li, Z. Chen, and R. S. Blum, "Low-rank tensor decomposition-aided channel estimation for millimeter wave MIMO-OFDM systems," *IEEE Journal Selected Areas in Communications*, vol. 35, no. 7, pp. 1524–1538, July 2017.
- [23] X. Li, J. Fang, H. Li, and P. Wang, "Millimeter wave channel estimation via exploiting joint sparse and low-rank structures," *IEEE Transactions on Wireless Communications*, vol. 17, no. 2, pp. 1123–1133, Feb 2018.
- [24] H. Hassanieh, O. Abari, M. Rodriguez, M. Abdelghany, D. Katabi, and P. Indyk, "Fast millimeter wave beam alignment," in *Proceedings of the 2018 Conference of the ACM Special Interest Group on Data Communication*, Budapest, Hungary, August 20-25 2018, pp. 432–445.
- [25] M. L. Moraveca, J. K. Romberg, and R. G. Baraniuk, "Compressive phase retrieval," *Proc. SPIE*, vol. 6701, p. 670120, 2007.
- [26] H. Ohlsson, A. Y. Yang, R. Dong, and S. Sastry, "CPRL-An extension of compressive sensing to the phase retrieval problem," in *Advances in Neural Information Processing Systems 25 (NIPS 2012)*, Lake Tahoe, Nevada, USA, Dec. 3-Dec. 6 2012, pp. 1367–1375.
- [27] Y. Shechtman, A. Beck, and Y. C. Eldar, "GESPAR: Efficient phase retrieval of sparse signals," *IEEE Transactions on Signal Processing*, vol. 62, no. 4, pp. 928–938, Feb. 2014.
- [28] S. Bahmani and J. Romberg, "Efficient compressive phase retrieval with constrained sensing vectors," in *Advances in Neural Information Processing Systems (NIPS)*, vol. 28, Montreal, Quebec, Canada, December 7-12 2015, pp. 523–531.
- [29] R. Pedarsani, D. Yin, K. Lee, and K. Ramchandran, "PhaseCode: Fast and efficient compressive phase retrieval based on sparse-graph codes," *IEEE Transactions on Information Theory*, vol. 63, no. 6, pp. 3663–3691, June 2017.
- [30] X. Song, S. Haghighatshoar, and G. Caire, "Efficient beam alignment for mmWave single-carrier systems with hybrid MIMO transceivers," *available at arXiv:1806.06425*, 2018.